Inorganic Chemistry

Article

pubs.acs.org/IC

The Missing Entry in the Agostic−Anagostic Series: Rh(I)−η^1-C Interactions in P(CH)P Pincer Complexes

Christine Lepetit,*[,†,‡] Jordi Poater,[§] M. Esmail Alikhani,*[,⊥,#] Bernard Silvi,*[,∥,¶] Yves Canac,[†,‡] Julia Contreras-García,[∥,¶] Miquel Solà,[§] and Remi Chauvin*[,†,‡]

[†]Laboratoire de Chimie de Coordination, CNRS, 205 route de Narbonne, BP 44099, F-31077 Toulouse Cedex 4, France

[‡]Université de Toulouse, UPS, INPT, F-31077 Toulouse Cedex 4, France

[§]Institut de Química Computacional i Catàlisi and Departament de Química, Universitat de Girona, Campus de Montilivi, 17071 Girona, Catalonia, Spain

[⊥]Sorbonne Universités, UPMC Univ. Paris 06, MONARIS, UMR 8233, Université Pierre et Marie Curie, 4 Place Jussieu, case courrier 49, F-75252 Paris Cedex 05, France

[#]CNRS, MONARIS, UMR 8233, Université Pierre et Marie Curie, 4 Place Jussieu, case courrier 49, F-75252 Paris Cedex 05, France

[∥]UPMC Univ. Paris 06, UMR 7616, Laboratoire de Chimie Théorique, F-75005 Paris, France

[¶]CNRS, UMR 7616, Laboratoire de Chimie Théorique, F-75005 Paris, France

Supporting Information

ABSTRACT: The missing entry, namely, the "C-anagostic" or η^1-C interaction, closing the agostic−anagostic series of metal−CH(aryl) interactions is found in a bis(amidiniophosphine) P(CH)P pincer rhodium complex. The three entries, namely, agostic η^2-(C,H), anagostic (related to hydrogen bonding, thus recoined here as "H-anagostic"), and C-anagostic interactions, are unambiguously characterized by electron localization function (ELF) topological analysis. Other theoretical tools such as noncovalent interaction (NCI) analysis and multicenter electron delocalization indices (MCIs) support the ELF characterization. A η^2-(C,H) agostic interaction is evidenced by a disynaptic V(C,H) or trisynaptic V(M,C,H) ELF basin with a significant quantum topological atoms in molecules (QTAIM) atomic contribution of the metal M and a large covariance (in absolute value) with the metal core basin C(M). The C-anagostic η^1-C interaction is characterized by a disynaptic V(M,C) basin, a weak covariance (in absolute value) of V(C,H) and C(M) populations, and a negligible QTAIM atomic contribution of M to V(C,H). The relevance of these ELF signatures is evidenced in a selected series of related rhodium and osmium complexes.

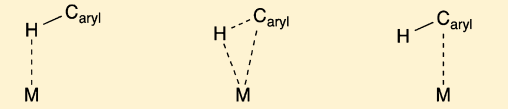

INTRODUCTION

In the family of carbeniophosphanes, amidiniophosphanes are α-cationic electron-poor ligands with versatile coordinating properties.[1] Whereas P,C,P-tridentate (PCP) pincer complexes with a single amidiniophosphine end facing a phosphinite opposite end were recently described in the nickel(II) series, PCP pincer complexes with two amidiniophosphine ends remain unknown.[2] In the rhodium(I) series, the PCP pincer complex **1** escaped all attempts of isolation, and only the P(CH)P pincer complex **2** could be obtained from the P,P-chelated precursor **3** (Scheme 1).[3] On the basis of density functional theory (DFT) studies, an alternative to the classical C−H oxidative addition pathway was proposed to explain the formation of **2** and its reluctance to yield the PCP pincer **1**.[3,4]

The nature of bonding in **2** remained to be elucidated. Experimental and calculated spectra of **2** are indicative of a weak rhodium−phenylene interaction.[3] The out-of-plane bending of the C1−H1 bond by 10° and the slight elongation of the C1−C2 and C1−C3 bonds are the main noticeable geometric characteristics. The ^{1}H NMR chemical shift of H1 is shifted downfield (9.81 ppm) with respect to the precursor complex **3** (8.70 ppm). This is in contrast with the strong ^{13}C NMR upfield shift of C1 from 124.8 to 111.4 ppm. From both experimental observations and natural bond order (NBO) analysis, especially using the Wiberg indices, a Rh−η^1-C1 bonding mode is anticipated with only secondary contributions from the geminal C2, C3, and H1 atoms (Scheme 1).[3]

Various types of metal−phenylene interactions are known. The η^6 coordination mode, reducing somewhat the aromatic character of the ring,[5] is the most current bonding mode, although η^4 and η^2 coordination modes are also known,[6] especially in the naphthylene series.[6e] The η^1 coordination mode has been only sparingly invoked (vide infra).

The η^1 coordination mode of benzene to the Ag cation of a crystallized carborane salt was postulated on the basis of a short Ag---C distance (2.4 Å).[7] A weak η^1-C coordination of the aromatic ring to the Rh center was suggested to stabilize the cationic complex **4**, isolated as an intermediate during computational studies of the oxidative addition pathway of

Received: January 9, 2015
Published: February 25, 2015

DOI: 10.1021/acs.inorgchem.5b00069
Inorg. Chem. 2015, 54, 2960−2969

Scheme 1. Structures of the Rhodium PCP Pincer Complex 1, P(CH)P Pincer Complex 2, and Chlorinated Precursor 3[3]

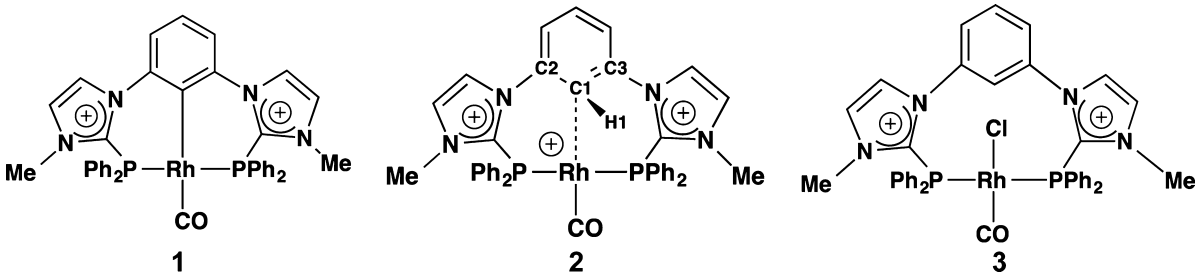

the agostic C1−H1 bond of complex **5** (Scheme 2).[8] A copper complex with structural and spectroscopic features comparable to those of **5** was initially described as agostic by Solà et al.[9] and finally described as a σ complex with a three-center three-electron interaction.[10] Similarly, in a palladium precatalyst for the amination of aryl chlorides, a highly asymmetric coordination mode to the Pd center, originally considered as η^1-C, was finally revised into a Pd−η^2-(C,H) coordination competing with a Pd−η^2-(C,C) olefin-like interaction.[11] Pregosin et al. claimed that there is weak η^1 π bonding in several ruthenium and palladium arene complexes, on the basis of a selective ^{13}C NMR upfield shift for only one of the six C atoms of the ring ($\delta_{^{13}C} \approx 105-112$ ppm vs the usual 127−130 ppm range for a free aromatic hydrocarbon).[12]

Scheme 2. Rhodium[8] and Osmium[21] Complexes Featuring Various Metal−CH(aryl) Interactions[a]

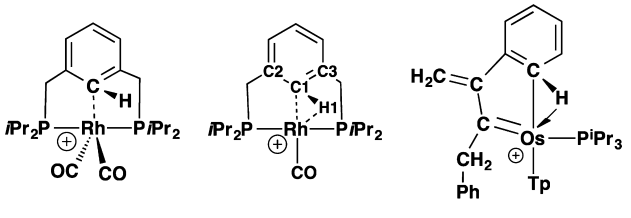

[a]Metal−ligand interactions are depicted as in the original reports.

Pregosin et al. claimed that there is weak η^1 π bonding in several ruthenium and palladium arene complexes, on the basis of a selective ^{13}C NMR upfield shift for only one of the six C atoms of the ring ($\delta_{^{13}C} \approx 105-112$ ppm vs the usual 127−130 ppm range for a free aromatic hydrocarbon).[12]

The above-mentioned ill-defined metal−phenylene interactions, claimed the η^1-C type, deserve classification. They might indeed be related to various metal−CH(aryl) interactions involving the geminal H atom, thus falling in the class of agostic C−H interactions. Such three-center two-electron interactions involving M−H−C groups were recently revisited and divided into the agostic and anagostic categories, with the latter being related to hydrogen bonding.[13]

Electron localization function (ELF) topological analysis[14] is a unique tool for chemical bonding analysis, especially for covalent or donor−acceptor interactions, because it provides a partition of the molecular space into basins that are in one-to-one correspondence with classical Lewis-type electronic units such as cores, bonds, and lone pairs.[15] The populations and (co)variances of these valence basins can be further interpreted in terms of weighted combinations of mesomeric structures.[16] In the ELF analysis framework, an agostic interaction would be characterized by a trisynaptic basin V(C,H,M) belonging to the valence shells of the three atoms,[17] which implies a sizable quantum topological atoms in molecules (QTAIM) atomic contribution (typically >0.1e) of the metal to the basin population and an absolute value of the covariance of the V(C,H,M) and C(M) basin populations comparable to that of V(M,H) and C(M) in hydrides, i.e., >0.2, for transition metals.

As far as weak metal−phenylene interactions are considered, noncovalent interaction (NCI) analysis[18] and multicenter electron delocalization indices (MCIs)[19] provide complementary information.

In this work, complexes **2**−**6**, representatives of various metal−CH(aryl) interactions (Schemes 1 and 2), are studied using these complementary theoretical approaches.

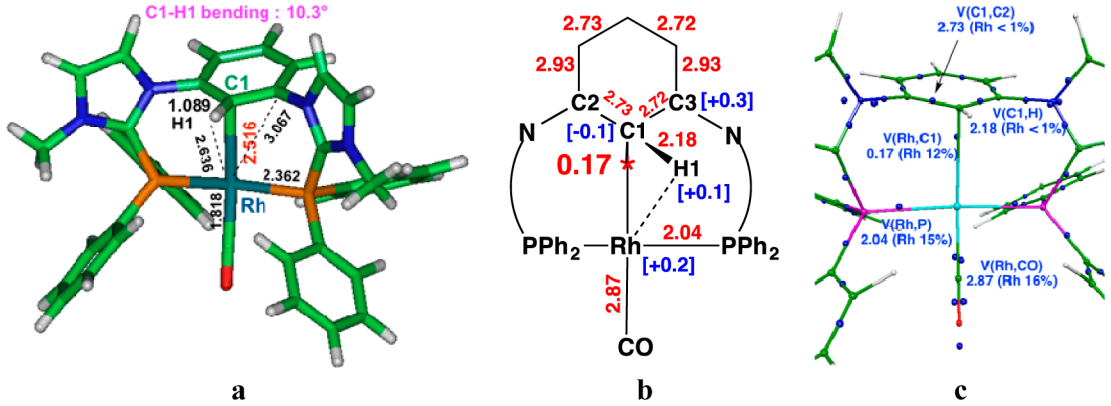

Figure 1. Calculated data for the tricationic P(CH)P pincer complex **2** of quasi-C_s symmetry. (a) Selected internuclear distances calculated at the PCM-B3PW91/6-31G**/LANL2DZ*(Rh) level in the acetonitrile solvent (ε = 35.688). (b) Average populations of selected ELF valence basins (in red) and QTAIM atomic charges continuum (in blue square brackets) calculated for **2** at the B3PW91/6-31G**/DGDZVP(Rh)//PCM-B3PW91/6-31G**/LANL2DZ*(Rh) level. (c) Map of ELF attractors of **2**. Valence attractors are in blue, and core attractors are atom-colored. The populations of selected disynaptic ELF basins and their rhodium QTAIM atomic contributions are also indicated.

DOI: 10.1021/acs.inorgchem.5b00069
Inorg. Chem. 2015, 54, 2960−2969

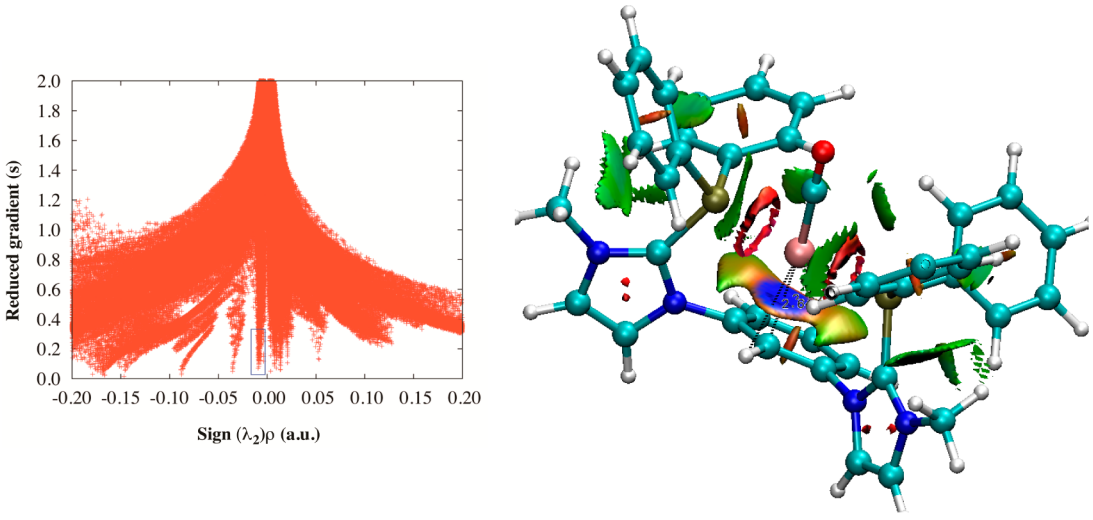

Figure 2. NCI analysis of the pincer rhodium complex **2** performed at the B3PW91/6-31G**/DGDZVP(Rh)//PCM-B3PW91/6-31G**/LANL2DZ*(Rh) level. (a) Two-dimensional plot of the reduced density gradient (s) versus the electron density ρ multiplied by the sign of the second Hessian eigenvalue (λ_2). (b) Three-dimensional plot of reduced gradient isosurfaces (s = 0.5).

RESULTS AND DISCUSSION

1. ELF and NCI Analysis of the Rhodium−Phenylene Interaction in Complex 2. The calculated structural characteristics of the weak rhodium−phenylene interaction suggested in the tricationic P(CH)P pincer complex **2** are first recalled hereafter (Figure 1a).[3] The Rh−C1 bond length (2.516 Å) is much shorter than the sum of the van der Waals (vdW) radii (3.70 Å) but longer than the sum of the covalent radii (2.10 Å).[3] The same holds for the Rh−C2 (3.056 Å) and Rh−C3 bond lengths (3.067 Å). The phenylene ring remains planar, suggesting that aromaticity is not dramatically affected by the interaction with the metal center. This is supported by the values of the nucleus independent chemical shift [NICS(1)] calculated at 1 Å above the geometric center of the ring, which are similar in complexes **2** [$NICS(1)_{zz}$ = −22.4 ppm] and **3** [$NICS(1)_{zz}$ = −21.5 ppm], where no rhodium−phenylene interaction is suspected. The out-of-plane bending of the C1−H1 bond by 10° and the slight elongation of the C1−C2 and C1−C3 bonds (see Scheme 1 for atom labeling) are also indicative of significant rhodium−phenylene interaction in **2**, which is further investigated hereafter using NCI and ELF topological analyses.

ELF Analysis. The electronic structure of **2** was further investigated using ELF topological analysis (Figures 1b,c). The core basin of rhodium C(Rh) is surrounded by five valence basins (Figure 1c). The disynaptic V(Rh,P) and V(Rh,CO) basins are related to the two Rh−P bonds and to the Rh−CO bond, respectively (Figure 1c).[20] The disynaptic V(Rh,C1) basin of very low population (0.17 e) may be assigned to weak Rh−η^1-C1 bonding. No localization domain is, however, visible between the Rh and C1 cores (see the ELF map in the Rh−C1−H1 plane; Figure S1 in the Supporting Information, SI). The low population of the V(Rh,C1) basin is almost insensitive to the accuracy level of the ELF analysis (grid size, approximation in gradient field analysis, etc.) and to the rhodium basis set (6-31G**, 6-311+G**, DGDZVP, and LANL2DZ*). The QTAIM atomic contribution of Rh to the V(Rh,C1) basin population is sizable (12%) and comparable with those of the V(Rh,P) (15%) and V(Rh,CO) (16%) basins. The V(Rh,C1) [respectively V(Rh,P)] attractor is located closer to C1 (respectively P) at about one-third of the Rh−C1 (respectively Rh−P) distance. The Rh−C1 and Rh−P bonds in complex **2** are, therefore, comparable in nature. The QTAIM atomic contribution of Rh to V(C1,H1) and V(C1,C2) is lower than 1%, suggesting the absence of interaction between the metal center and geminal C2, C3, and H1 atoms.

Both populations of the valence ELF basins and the QTAIM charges of the C atoms of the phenylene ring are in favor of a small change in the aromatic character of the ring (vide supra; Figure 1b).

NCI Analysis. NCI analysis relies on the electron density ρ and its reduced gradient $s(\rho) = \{1/[2(3\pi^2)^{1/3}]\}|\nabla\rho|/\rho^{4/3}$ to discriminate between various types of nonbonding interactions, namely, attractive, vdW-dispersive, and repulsive ones.[18] NCI analysis of **2** was performed at the B3PW91/6-31G**/DGDZVP(Rh)//PCM-B3PW91/6-31G**/LANL2DZ*(Rh) level of calculation, and the two-dimensional plot of the reduced gradient s versus $\text{sign}(\lambda_2)*\rho$, where λ_2 is the second Hessian eigenvalue, is shown in Figure 2a. It exhibits one spike in the region of low density (ρ = 0.88 au), highlighted by a blue frame, a typical signature of an attractive interaction.[18] When these points are plotted in real space, a blue discoidal reduced density gradient isosurface is visible on the three-dimensional plot of Figure 2b, from which an attractive interaction between Rh and C1 is suggested. It is centered on the Rh−C1 axis with a slight extension toward the C1−H1 bond, compatible with a very weak attractive interaction between Rh and C1 or between Rh and the C1−H1 bond, raising the question of other contributions to the rhodium−phenylene interaction than the Rh−η^1-C1 bonding evidenced above by ELF analysis. In the same line, NBO signatures of very weak donor−acceptor interactions were indeed found in **2** from second-order perturbative analysis, i.e., a stabilizing π(C1−C2) → 5s*(Rh) contribution of 5.5 kcal/mol and a stabilizing σ(C1−H1) → 5s*(Rh) contribution of 1.8 kcal/mol,[3] albeit close to the accuracy limit of NBO analysis.

It is worth noting that vdW-dispersive interactions between the phenyl phosphorus substituents of the amidiniophosphine

DOI: 10.1021/acs.inorgchem.5b00069
Inorg. Chem. 2015, 54, 2960−2969

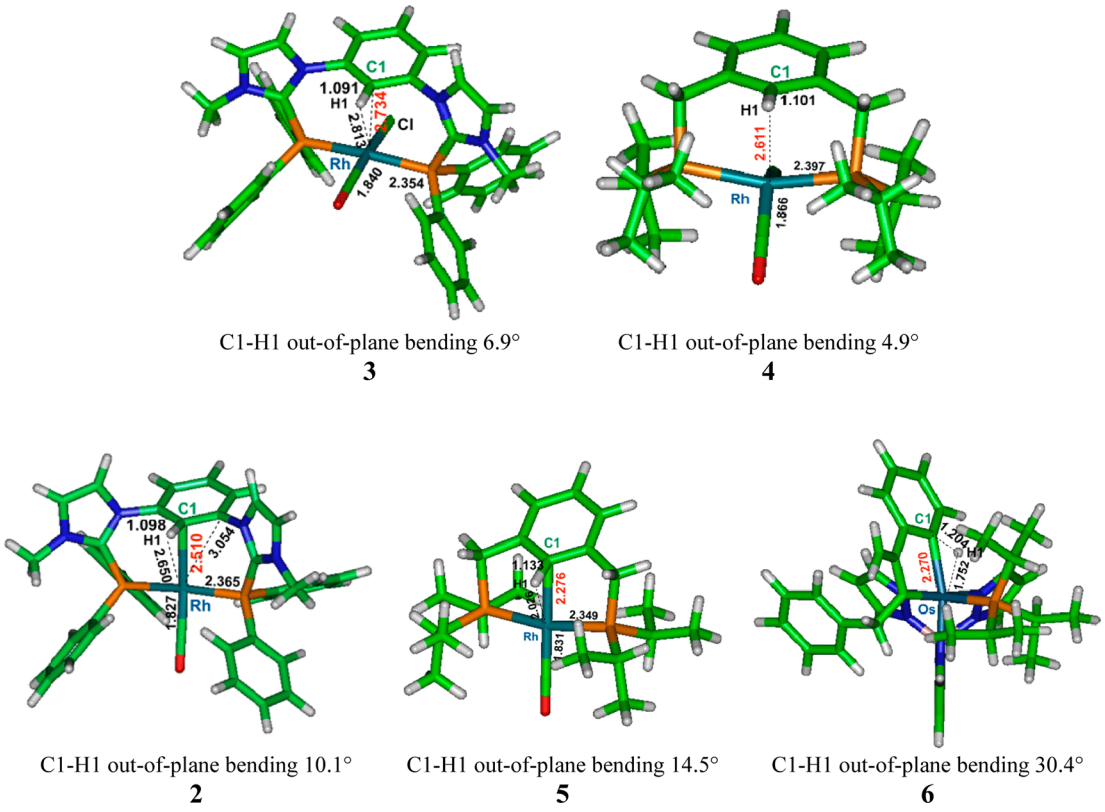

Figure 3. Structures and selected geometrical data for complexes **2**–**6** calculated at the PBE-D3/6-31G**/LANL2DZ*(M) level, where M = Rh or Os. Calculations under C_s symmetry constraint except for the osmium complex **6**.

Table 1. ELF Analysis of Complexes 2–6[a]

	V(M,C1)	% M[b]	Cov[c]	Vol[d]	M–C1	V(C1,H1)	% M[b]	Cov[e]	C1–H1 (Å)	bending[f]
3					2.734	2.19	0.00	−0.04	1.091	6.9
4					2.611	2.17	0.01	−0.05	1.101	4.9
2	0.21	0.01	−0.02	4.03	2.510	2.20	0.01	−0.06	1.098	10.1
5	0.38	0.04	−0.05	8.39	2.276	2.17	0.05	−0.15	1.133	14.5
p-NH_2-**5**	0.74	0.10	−0.11	15.60	2.247	2.14	0.03	−0.11	1.121	21.0
5′					2.280	2.46	0.09	−0.24	1.152	17.2
6					2.270	2.64[g]	0.16	−0.38	1.204	30.4

[a]B3PW91/6-31G**/LANL2DZ*(M)//PBE-D3/6-31G**/LANL2DZ*(M) level of calculation. Distances are in angstroms. [b]QTAIM atomic contribution of the metal M (e). [c]Covariance of populations of V(M,C1) and C(M). [d]Volume of V(M,C1) in bohr.[3] [e]Covariance of populations of V(C1,H1) and C(M). [f]Out-of-plane bending of C1–H1 in degrees. [g]Value referring to V(Os,C1,H1) instead of V(C1,H1).

ligands, as expected from the observed distances, are also visible as green isosurfaces (Figure 2b).

2. Theoretical Analysis of the Rhodium–Phenylene Interaction in the Series of Complexes 3–6. The nature of the metal–phenylene interaction was further investigated in a series of rhodium and osmium complexes, using various theoretical analysis tools.

The neutral chlorinated precursor **3** is taken as the reference for the absence of metal–phenylene interaction. The cationic rhodium carbonyl complexes **4** and **5** are selected respectively for the weak η^1-C and the η^2-(C,H) agostic interaction claimed by Milstein et al.[8] Finally, the cationic osmium complex **6** is selected as a representative of a strong agostic η^2-(C,H) interaction (Scheme 2).[21]

Geometries. Experimental structures are available for all of the selected complexes, except for complex **4**. However, large uncertainties are expected for the experimental C1–H1 bond lengths, and more reliable values must be sought from calculated structures. Because standard functionals, such as B3PW91, are not expected to properly describe weak (nonbonding) interactions,[22] various dispersion correction schemes for DFT were therefore evaluated for their ability to describe complexes **3** and **6**, for which accurate experimental data are available (Table S1 in the SI). The latest S12 dispersion correction scheme was also tested.[23]

Whatever the calculation level, the Rh–P, Rh–Cl, and P–C bond lengths of complex **3** are always overestimated compared to the experimental acceptable range (Table S1 in the SI). Only the B3PW91, PBE-D, and PBE-D3 functionals are able to predict an acceptable Rh–C1 bond distance. Finally, the gas-phase calculations of complex **6** using the B3PW91 and PBE-D3 functionals yield structures in best agreement with the experimental structure. It is worth noting that, at these levels of calculation, taking into account the acetonitrile solvent as a continuum has little effect.

DOI: 10.1021/acs.inorgchem.5b00069
Inorg. Chem. 2015, 54, 2960–2969

PBE-D3, including empirical dispersion corrections (DFT-D), was therefore selected as the most reliable functional, although B3PW91 results are also quite satisfactory (Table S1 in the SI). The structures of complexes **2**−**6** were therefore calculated at the PBE-D3/6-31G**/LANL2DZ*(M) level, where M = Rh or Os, under C_s symmetry constraint except for **6**.

Complexes **3** and **4** were found to exhibit the longest Rh−C1 bond distances (2.734 and 2.611 Å, respectively), a planar phenylene ring, and a slight out-of-plane bending of the C1−H1 bond (Figure 3), reflecting the weakness of the interaction between the rhodium and the phenylene ring. The out-of-plane bending of the C1−H1 bond increases from 10° in **2** up to 30° in **6**, simultaneously with the shortening of the M−C1 distance (M = Rh or Os) down to 2.270 Å and the lengthening of the C1−H1 bond up to 1.204 Å (Table 1), indicating the strengthening of the metal−phenylene interaction over the series **2**, **5**, and **6**.[24] It is noticeable that the normal to the phenylene ring plane is also orthogonal to the quasi-linear P−Rh−P axis in complexes **2**−**4**. However, this normal is tilted out from the P−Rh−P axis in complexes **5** and **6** by 37° and 58°, respectively, as expected in intermediates on the C1−H1 oxidative addition pathway. The metal−phenylene interactions are therefore of markedly different nature in complexes **2**−**4** and complexes **5** and **6**.

ELF Analysis. ELF analysis of complexes **2**−**6** was performed at the B3PW91/6-31G**/LANL2DZ*(M)//PBE-D3/6-31G**/LANL2DZ*(M) level of calculation (M = Rh or Os; Table 1 and Figures 4 and 5). The pseudopotential is required

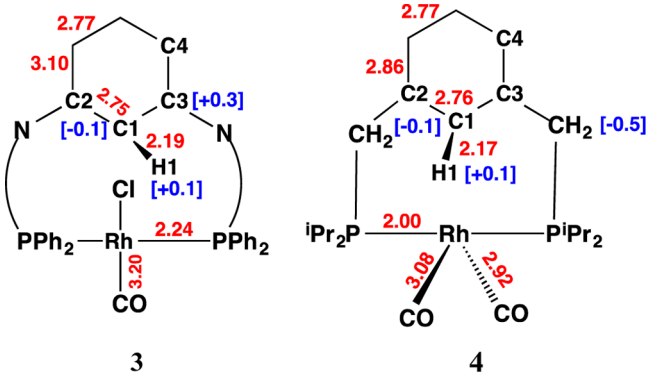

Figure 4. Average populations of selected ELF valence basins (in red) and QTAIM atomic charges (in blue square brackets) calculated for complexes **3** and **4** at the B3PW91/6-31G**/LANL2DZ*(Rh)//PBE-D3/6-31G**/LANL2DZ*(Rh) level under C_s symmetry constraint.

for a suitable description of the electronic structure of the osmium complex **6**. At this level, ELF analysis of **2** is very similar to the results previously obtained at the B3PW91/6-31G**/DGDZVP(Rh)//PCM-B3PW91/6-31G**/LANL2DZ*(Rh) level of calculation (Figure 1b,c).

For complexes **3** and **4**, no valence attractor is found between Rh and C1 (Figure 4), ruling out any significant electron-sharing interaction between those atoms. The QTAIM atomic contribution of Rh to the disynaptic V(C1,H1) basin and the covariance of the populations of the V(C1,H1) and C(Rh) basins are also negligible (Table 1), ruling out any significant electron-sharing interaction between Rh and (C1 or H1).

In contrast, for complexes **2** and **5**, the disynaptic V(Rh,C1) attractor (ELF = 0.7) is indicative of an electron-sharing interaction of the Rh−η^1-C type (Figure 5). The population of

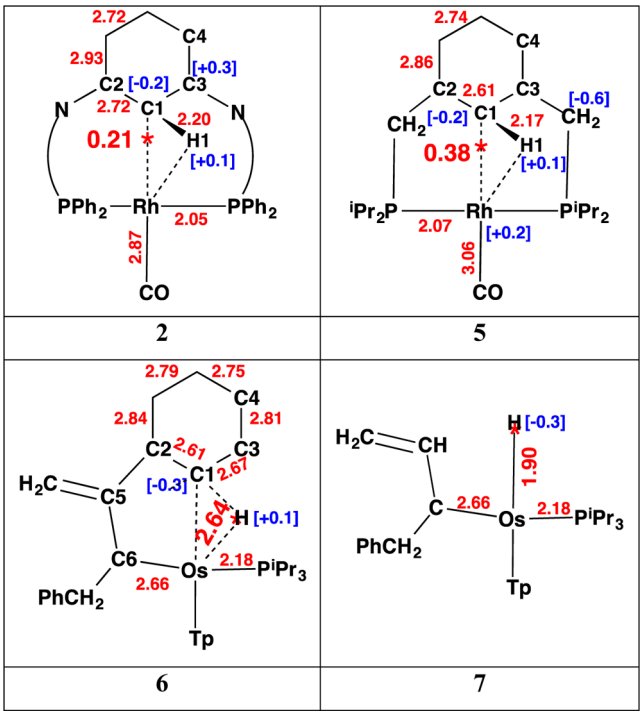

Figure 5. Average populations of selected ELF valence basins (in red) and QTAIM atomic charges (in blue square brackets) calculated at the B3PW91/6-31G**/LANL2DZ*(M)//PBE-D3/6-31G**/LANL2DZ*(M) level for complexes **2** and **5**−**7**. C_s symmetry constraint for **2** and **5**.

the V(Rh,C1) basin in the monocationic complex **5** is low (0.38 e) but almost twice that in the tricationic complex **2** (0.21 e). The same holds for the volume of the basin (Table 1). The QTAIM atomic contribution of Rh to V(Rh,C1) is weak, namely, 0.01 and 0.04 e for **2** and **5**, respectively (Table 1). The delocalization between V(Rh,C1) and C(Rh) is rather small because the absolute value of the covariance of their populations is small, 0.02 and 0.05 for **2** and **5**, respectively, indicating, together with the QTAIM atomic contributions, a mostly electrostatic interaction between these basins, in agreement with the attractive interaction found with NCI analysis (Figure 2).

The ELF picture of the osmium complex **6** exhibits a trisynaptic V(Os,C1,H1) basin with a large population of 2.64 e (Figure 5). The absolute value of the covariance of the populations of V(Os,C1,H1) and C(Os) (0.38) is large as well as the QTAIM atomic contribution of Os to V(Os,C1,H1), namely, 0.16 e (Table 1). The ELF topology is thus in agreement with the strong Os−η^2-(C1,H1) α-agostic interaction previously reported.[21]

Although the trisynaptic attractor V(Os,C1,H1) is located in very close proximity of H1, the ELF topology of **6** is clearly different from the one expected for an osmium hydride such as complex **7**, a model hydride derived from complex **6**, exhibiting a disynaptic V(Os,H1) basin (Figure 5 and Table S2 in the SI).

While the QTAIM atomic contribution of Rh to the disynaptic V(C1,H1) basin of **2** is negligible (0.01 e), it is sizable for **5** (0.05 e). Similarly, the absolute value of the covariance of the populations of V(C1,H1) and C(Rh) is weak in **2** (0.06) but is large in **5** (0.15) (Table 1). In the latter complex **5**, beyond the major Rh−η^1-C1 interaction charac-

DOI: 10.1021/acs.inorgchem.5b00069
Inorg. Chem. 2015, 54, 2960−2969

terized by the disynaptic V(Rh,C1) basin, a sizable contribution of Rh−η^2-(C1,H1) α-agostic interaction therefore takes place.

It is therefore possible to discriminate between η^1-C and η^2-(C,H) α-agostic bonding using ELF analysis: (i) a disynaptic V(C,H) or trisynaptic V(M,C,H) basin with a significant QTAIM atomic contribution of the metal M and a large covariance in the absolute value with C(M) are the ELF signature of a η^2-(C,H) α-agostic interaction; (ii) a disynaptic V(M,C) basin, a weak covariance of the populations of V(C,H) and C(M), and a negligible QTAIM atomic contribution of the metal M to V(C,H) are the ELF signature of a η^1-C interaction.

The relative contribution of η^1-C and η^2-(C,H) bonding modes in the series of complexes **2**−**6** was also investigated by inspection of the tilting angle of the normal to the phenylene ring with the Rh−CO (or Os−Tp) axis (Figure 5). The deviation from alignment of both axes is expected to be related with the contribution of the η^2-(C,H) bonding mode in the complex, which may be considered as an intermediate on the C1−H1 oxidative addition pathway. The tilting angle is estimated from the C4−C3−N−P dihedral angle in complexes **2** and **3**, by the C4−C3−C−P dihedral angle in complex **4** and in the derivatives of **5**, and by the C1−C2−C5−C6 dihedral angle in **6** (see labeling in Figure 5). These dihedral angles are expected to take the value of 90° for the perfect alignment of both axes. This is almost the case in **2** (102.7°), **3** (102.4°), **4** (107.7°), and *p*-NH_2-**2** (113.9°), suggesting a negligible contribution of η^2-(C,H) bonding in these complexes, in agreement with the related ELF analyses (Table 1). In contrast, the C4−C3−C−P dihedral angles are much larger, thus indicating significant deviation from alignment in *p*-NH_2-**5** (132.5°), **5** (126.7°), **5′** (136.0°; vide infra for the definition of the **5′** structure), and **6** (147.7°), in agreement with the corresponding increasing contribution of η^2-(C,H) bonding evidenced using ELF analysis (Table 1).

The rhodium−phenylene interaction in **2** may therefore be described by resonance between three mesomeric forms (Figure 6a). According to the population of the V(Rh,C) basin, the weight of the mesomeric forms accounting for η^1-C bonding is about 10%.[16a] The strong η^2-(C,H) α-agostic interaction of complex **6** may be described by resonance between the mesomeric forms of Figure 6b with a nonzero but weak weight of the C−H oxidative addition form.

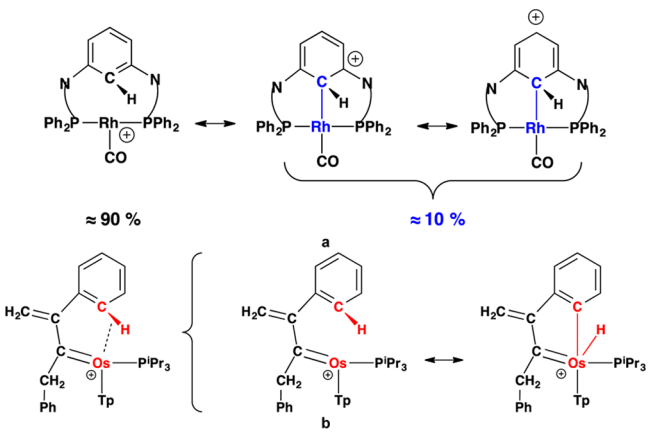

Figure 6. (a) Most representative mesomeric forms of the rhodium−phenylene interaction in complex **2**. Only the N and P atoms of the imidazoliophosphine peripheral extremities connected to the Rh center are shown. (b) Mesomeric forms describing Os−η^2-(C,H) agostic bonding in complex **6**. The dotted line is not a Lewis symbol but is intended to indicate the weak-bonding feature.

The relative contribution of Rh−η^1-C and Rh−η^2-(C,H) α-agostic bonding can be tuned by substitution of the phenylene ring or by electronic enrichment of the Rh center of complexes **2** and **5**. On the basis of the mesomeric description of Figure 6, para substitution of the phenylene ring with π-donor groups (+M) is expected to favor η^1-C bonding, while electron enrichment of the metal center is expected to favor η^2-(C,H) α-agostic bonding.

Para substitution of the phenylene ring by NH_2 (Figure 7) results in enhancement of the η^1-C contribution in *p*-NH_2-**5**, while substitution of the CO ligand at the Rh center by PMe_3 allows for increases of the η^2-(C,H) α-agostic bonding contribution in **5′** (Tables 1 and S2 and S3 in the SI).

The effect of phenylene substitution may be related to that occurring in electrophilic aromatic substitution (Holleman's rules).[25] Upon para substitution of the phenylene ring of **2** and **5** with π donors (+M) such as amino (NH_2) or methoxy (OMe) groups or even halogens (F, Cl), the population of V(Rh,C1) increases (Tables S2−S4 in the SI), as anticipated from the mesomeric forms displayed in Figure 8a. The contribution of η^1-C bonding therefore increases and the corresponding localization domain, hardly visible on the ELF map of **5** (black arrow in Figure S1 in the SI), becomes clearly visible on the ELF map of *p*-NH_2-**5** (Figure 7a) or in the ELF = 0.81 isosurface of Figure 7b.

The reverse situation occurs upon meta substitution of the phenylene ring with X = OMe, F, Cl, or CF_3. The population of V(Rh,C1), i.e., the contribution of η^1-C bonding, decreases in the corresponding derivatives of **2** and **5** (Tables S2−S4 in the SI). The η^2-(C,H) α-agostic bonding contribution increases conversely in the corresponding complexes X-**5**. The same holds upon para substitution of the phenylene ring of **5** with the electron-withdrawing group X = NO_2.

Upon meta substitution of the phenylene ring with π-donor groups, the weight of the zwitterionic mesomeric form shown in Figure 8b is expected to increase. This form is indeed in favor of the electronic enrichment of the diphosphine ligand, expected to enhance back-donation from the Rh d orbital to the σ*(C−H) orbital, thus the contribution of η^2-(C,H) α-agostic bonding. The mesomeric effect (+M) of π-donor substituents is dominant over their inductive effect (−I).

It is noticeable that, whatever the substitution pattern (nature and position of the substituent) in the bis(amidiniophosphine) pincer complex **2**, η^1-C bonding is the only contribution to the rhodium−phenylene interaction.

MCIs. Three- and two-center electron delocalization indices were calculated at the B3PW91/6-31G**/LANL2DZ*(M)//PBE-D3/6-31G**/LANL2DZ*(M) level (Table 2). These indices quantify the electron sharing between the atoms involved in the index.

The two-center delocalization indices, DI(C1,M), are naturally related to η^1-C bonding. These indices increase from 0.19 (non-bonded Rh and C1 atoms in complexes **3** and **4**) to 0.26 in complex **2** and up to 0.4−0.5 for strongly bonded Rh and C1 atoms in **5** and **6**. On the basis of the above ELF analysis, a threshold of 0.2 may be retained as a criterion for the existence of η^1-C bonding.

Agostic bonds are defined as three-center two-electron interactions, and, consequently, a large three-center index, MCI(H1,C1,M), may be related to η^2-(C1,H1) α-agostic bonding. Indeed, this index increases along the series **3** < **2** ≈ **4**

DOI: 10.1021/acs.inorgchem.5b00069
Inorg. Chem. 2015, 54, 2960−2969

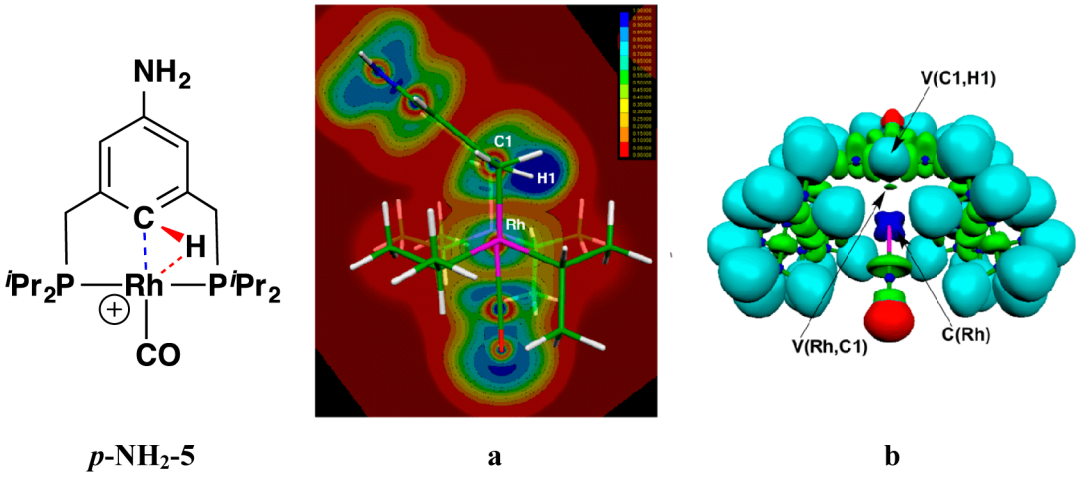

Figure 7. C_s-symmetric complex *p*-NH_2-**5**: (a) ELF map in the Rh−C1−H1 plane; (b) localization domains (ELF = 0.81). B3PW91/6-31G**/LANL2DZ*(Rh)//PBE-D3/6-31G**/LANL2DZ*(Rh) level of calculation.

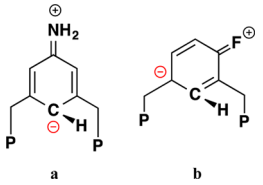

Figure 8. Mesomeric forms of the phenylene ring accounting for the π-donor substituent effect (+M) in complexes X-**5**. (a) X = NH_2: para substitution of the phenylene ring favoring η^1-C bonding. (b) X = F: meta substitution of the phenylene ring favoring η^2-(C,H) bonding via electronic enrichment of the diphosphine.

Table 2. Three-Center Electron Delocalization Indices (MCIs) and Two-Center Electron Delocalization Indices (DIs): B3PW91/6-31G/LANL2DZ*(M)//PBE-D3/6-31G**/LANL2DZ*(M) Level of Calculation**

	3	4	2	5	6
MCI(C1,C2,M)	0.008	0.019	0.033	0.031	0.013
MCI(H1,C1,M)	0.013	0.022	0.020	0.067	0.088
DI(H,M)	0.075	0.182	0.127	0.340	0.550
DI(C1,M)	0.189	0.197	0.255	0.405	0.474
DI(H1,C1)	0.955	0.965	0.962	0.844	0.689

< **5** < **6**. For the titanium complex $(Me_2PCH_2CH_2PMe_2)$-$TiEtCl_3$ formerly studied at the same level as in the present work,[13] MCI(Ti,H,C) = 0.044. The reference for the less common η^2-(C,C) agostic interactions can be taken from the complex $[Rh(P^iPr_3)(C_{14}H_{16})][BAr^F{}_4]$.[26] In this case, MCI-(Rh,C,C) = 0.058. The latter complex also presents a Rh−η^2-(C,H) agostic interaction, with MCI(Rh,H,C) = 0.045, almost equal to that found in the above titanium complex. Taking into account these reference systems, a threshold of 0.040 can be retained as the three-center delocalization index criterion for an agostic interaction. MCI(C1,C2,M) of complexes **2**−**4** are therefore in favor of the absence of such agostic interaction. On the other hand, MCI(H1,C1,M) values of 0.067 and 0.088 for complexes **5** and **6**, respectively, are consistent with a sizable and strong η^2-(C1,H1) α-agostic interaction, respectively, in agreement with the above ELF analysis.

CONCLUSIONS

The metal−phenylene interaction in the series of complexes **2**−**6** was characterized using ELF analysis. η^1-C bonding only, referred to as C-anagostic interaction, was evidenced in complex **2**. Previous claims might be refined according to Scheme 3.[8,21] No Rh−C electron-sharing interaction is indeed found in **4**, while Rh−η^1-C bonding occurs with concomitant α-agostic η^2(C,H) bonding in **5**. In agreement with previous reports, ELF analysis is clearly indicative of a strong α-agostic Os−η^2(C,H) interaction in **6**.

The electron-poor peripheral amidiniophosphine extremities of the P(CH)P pincer complex **2**[1] allowed for isolation and characterization of the η^1-C (or C-anagostic) bonding mode. In contrast, the η^1-C bonding mode exists along with the α-agostic η^2-(C,H) bonding in the pincer complex **5**, which was built from standard electron-rich phosphine peripheral extremities. Electronic enrichment of **5** by substitution of CO with PMe_3 at the metal center leads to exclusive α-agostic η^2-(C,H) bonding in **5′**. The rhodium−phenylene interaction vanishes in **4**, upon the addition of a CO ligand to **5**. This suggests that this second CO ligand does not act as the usual strong π acceptor, expected

Scheme 3. Bonding Types in the Series of Complexes 2−6[a]

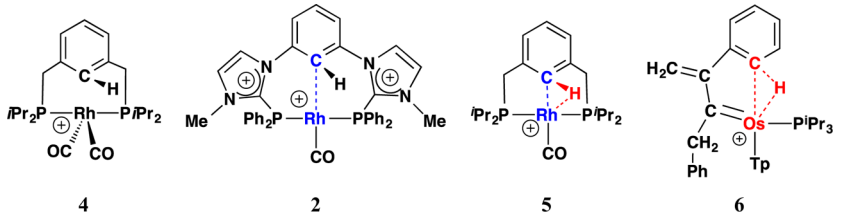

[a] η^1-C (or C-anagostic) bonding is highlighted in blue, while α-agostic η^2-(C,H) bonding is highlighted in red.

DOI: 10.1021/acs.inorgchem.5b00069
Inorg. Chem. 2015, 54, 2960−2969

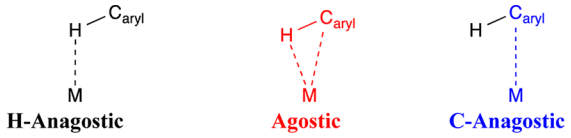

	H-Anagostic	Agostic	C-Anagostic
ELF	V(C,H) Cov (V(C,H), C(M)) ≈ 0	V(C,H) or **V(M, C, H)** Large absolute value of covariance with C(M)	V(C,H) + **V(M,C)** Cov (V(C,H), C(M)) ≈ 0
MCI	3c-ESI ≈ 0 or < 0	3c-ESI > 0.040	3c-ESI≈ 0, DI(C,M) > 0.2

Figure 9. Complete typology of metal−CH(aryl) interactions and corresponding ELF and MCI signatures.

to hinder C−H oxidative addition[8,27] but rather increases the electron density of the metal center. Several examples of such unusual behavior of the CO ligand have been reported.[8,28] The relative contribution of the η^1-C and η^2-(C,H) bonding types results therefore from a subtle balance between various electronic effects in the coordination sphere of the metallic center.

η^1-C (or C-anagostic) bonding may be considered as the missing entry in the typology of metal−CH(aryl) interactions besides agostic η^2-(C,H) and H-anagostic interactions (i.e., hydrogen bonding to the metal center) with clear-cut ELF and MCI characterization (Figure 9).

An agostic or η^2-(C,H) interaction is characterized by a disynaptic V(C,H) or trisynaptic V(C,H,M) ELF basin, with an absolute value of the covariance of the valence and core C(M) basin populations larger than 0.2. For the H-anagostic interaction, the metal QTAIM atomic contribution to V(C,H) is expected to be negligible and the absolute value of the covariance between the V(C,H) and C(M) basin populations of the order of magnitude of that found in ionic compounds or hydrogen-bonded complexes, namely, lower than 0.2. Finally, the C-anagostic interaction or η^1-C bonding mode gives rise to a V(C,M) disynaptic basin, and the absolute value of the covariance between the V(C,H) and C(M) populations is negligible.

The structures depicted in Figure 9 might be a priori interpreted as limiting mesomeric (or valence-bond) forms applied to any type of metal−CH complexes with specific weights. A geometry-based scheme for the weighting of the C- and H-anagostic forms might be naturally envisaged.[29]

C-anagostic bonding might be considered as a key feature of the intermediate of C−H activation, in alternative pathways to the typical C−H oxidative addition at electron-rich transition-metal centers of low valency.[3,4]

Future work will focus on the further use of ELF analysis for the elucidation of other ill-defined metal−phenylene interactions that may involve C-anagostic interactions such as in recently reported complexes of benziporphyrins.[30]

COMPUTATIONAL METHODS

Geometries were fully optimized at various DFT levels using *Gaussian09*.[31] Vibrational analysis was performed at the same level as geometry optimization. In the PCM-B3PW91/6-31G**/LANL2DZ*(M) (M = Rh or Os) notation, LANL2DZ*(M) means that f-polarization functions derived by Ehlers et al.[32] for M have been added to the LANL2DZ(M) basis set and that solvent effects were included using the polarizable continuum model (PCM) implemented in *Gaussian09* for acetonitrile (ε = 35.688).

Calculations with functionals including (long-range) dispersion corrections were performed using *Gaussian09*[31] or the *ADF2013* package.[33] In the latter case, the geometries of the rhodium complexes were fully optimized using the PBE functional in combination with Slater-type (STO) all-electron basis sets of TZP quality including scalar relativistic effects.[34] Vibrational analysis was performed at the same level as the geometry optimization. Solvent effects were included using the conductor-like screening model (COSMO)[35] implemented in *ADF2013*.[33]

ELF[14] and QTAIM[15b,36] topological analyses were performed with the *TopMoD* package.[37] ELF maps were plotted using the *Molekel* program.[38]

MCIs are derived from the first multicenter index, the I_{ring} index, which was defined by Giambiagi as

$$I_{ring}(\mathbf{A}) = 2^n \sum_{i_1,i_2,i_3,\ldots,i_n}^{occ} S_{(i_1 i_2)}(A_1)\, S_{(i_2 i_3)}(A_2) \ldots S_{(i_n i_1)}(A_n) \quad (1)$$

where $S_{ij}(A_k)$ is the overlap between occupied molecular orbitals i and j within the domain of atom k. In this formula, it is considered that the ring is formed by atoms in the string $\{\mathbf{A}\} = \{A_1, A_2, \ldots, A_n\}$ and I_{ring} is considered a measure of the simultaneous electron sharing between the atoms. For the particular case $n = 2$, I_{ring} is identical with the two-center electron delocalization index. Extension of this I_{ring} index of Giambiagi by Bultinck and co-workers resulted in the so-called MCI[39]

$$\mathrm{MCI}(\mathbf{A}) = \frac{1}{2n} \sum_{P(\mathbf{A})} I_{ring}(A) \quad (2)$$

where $P(\mathbf{A})$ stands for the $n!$ permutations of the elements in the string $\{\mathbf{A}\}$. In this work, MCI is calculated for the three members involved in the metal−CH(aryl) or metal−CC(aryl) interaction. The numerical integrations over the atomic domains were carried out within the "fuzzy atom" framework using the Becke ρ partitioning scheme[40] with the *APOST-3D* program.[41] DI, I_{ring}, and MCI indices were obtained with the *ESI-3D* program.[42]

NCI analysis was carried out with the *NCIPLOT* program.[18b] A density cutoff of ρ = 0.1 au was applied, and the pictures were created for an isosurface value of s = 0.5 and colored in the [−0.03, 0.03] au sign(λ_2)ρ range. This kind of approach and these values are especially suitable to reveal both very weak and stronger NCIs that might be blind to the AIM approach.[43]

ASSOCIATED CONTENT

Supporting Information

Geometrical data used for calibration of the calculation method (Table S1) and for the geometrical analysis described in ref 29 (Table S5) and complete ELF topological characterization of complexes **2**−**6** and of their derivatives (Figure S1 and Tables S2−S4). This material is available free of charge via the Internet at http://pubs.acs.org.

AUTHOR INFORMATION

Corresponding Authors

*E-mail: christine.lepetit@lcc-toulouse.fr. Fax: (+33) 5 61 55 30 03.

DOI: 10.1021/acs.inorgchem.5b00069
Inorg. Chem. 2015, 54, 2960−2969

*E-mail: esmail.alikhani@upmc.fr.
*E-mail: silvi@lct.jussieu.fr.
*E-mail: remi.chauvin@lcc-toulouse.fr. Fax: (+33) 5 61 55 30 03.

Notes

The authors declare no competing financial interest.

■ ACKNOWLEDGMENTS

The theoretical studies were performed using HPC resources from CALMIP (Grant 2011-2013[0851]) and from GENCI-[CINES/IDRIS] (Grant 2011-2013[085008]). J.P. and M.S. are grateful to the following organizations for financial support: the Ministerio de Ciencia e Innovación (Projects CTQ2011-23156/BQU and CTQ2011-25086/BQU) and the Generalitat de Catalunya (Projects 2014SGR931, 2009SGR528, and 2009SGR637; AIRE-CTP2012 fellowship for J.P.; 2014 ICREA Academia prize for excellence in research funded by the DIUE for M.S.).

■ REFERENCES

(1) Canac, Y.; Maaliki, C.; Abdellah, I.; Chauvin, R. *New J. Chem.* **2012**, *36*, 17−27.
(2) Vabre, B.; Canac, Y.; Duhayon, C.; Chauvin, R.; Zargarian, D. *Chem. Commun.* **2012**, *48*, 10446−10448.
(3) Barthes, C.; Lepetit, C.; Canac, Y.; Duhayon, C.; Zargarian, D.; Chauvin, R. *Inorg. Chem.* **2013**, *52*, 48−58.
(4) Vabre, B.; Lambert, M. L.; Petit, A.; Ess, D. H.; Zargarian, D. *Organometallics* **2012**, *31*, 6041−6053.
(5) Feixas, F.; Jiménez-Halla, J. O. C.; Matito, E.; Poater, J.; Solà, M. *Polish J. Chem.* **2007**, *81*, 783−797.
(6) (a) Silverthorn, W. E. *Adv. Organomet. Chem.* **1975**, *13*, 47−137. (b) Lepetit, C.; Kermarec, M.; Che, M. *Colloids Surf. A* **1993**, *72*, 265−274. (c) Garrot, J.-M.; Lepetit, C.; Che, M. *J. Mol. Catal.* **1996**, *107*, 137−143. (d) Filipuzzi, S.; Pregosin, P. S.; Calhorda, M. J.; Costa, P. J. *Organometallics* **2008**, *27*, 2949−2958. (e) Soleilhavoup, M.; Viau, L.; Commenges, G.; Lepetit, C.; Chauvin, R. *Eur. J. Inorg. Chem.* **2003**, 207−212.
(7) Shelly, K.; Finster, D. C.; Lee, Y. J.; Scheidt, W. R.; Reed, C. A. *J. Am. Chem. Soc.* **1985**, *107*, 5955−5959.
(8) (a) Montag, M.; Schwartsburd, L.; Cohen, R.; Leitus, G.; Ben-David, Y.; Martin, J. M. L.; Milstein, D. *Angew. Chem., Int. Ed.* **2007**, *46*, 1901−1904. (b) Montag, M.; Efremenko, I.; Cohen, R.; Shimon, L. J. W.; Leitus, G.; Diskin-Posner, Y.; Ben-David, Y.; Salem, H.; Martin, J. M. L.; Milstein, D. *Chem.—Eur. J.* **2010**, *16*, 328−353.
(9) Ribas, X.; Xifra, R.; Parella, T.; Poater, A.; Solà, M.; Llobet, A. *Angew. Chem., Int. Ed.* **2006**, *45*, 2941−2944.
(10) Ribas, X.; Calle, C.; Poater, A.; Xifra, R.; Casitas, A.; Gómez, L.; Parella, T.; Benet-Buchholz, J.; Schweiger, A.; Mitrikas, G.; Solà, M.; Llobet, A.; Stack, T. D. P. *J. Am. Chem. Soc.* **2010**, *132*, 12299−12306.
(11) Christmann, U.; Pantazis, D. A.; Benet-Buchholz, J.; McGrady, J. E.; Maseras, F.; Vilar, R. *J. Am. Chem. Soc.* **2006**, *128*, 6376−6390.
(12) (a) Geldbach, T. J.; Drago, D.; Pregosin, P. S. *J. Organomet. Chem.* **2002**, *643*−*644*, 214−222. (b) Geldbach, T. J.; Pregosin, P. S. *Eur. J. Inorg. Chem.* **2002**, *46*, 1907−1918. (c) Pregosin, P. S. *Chem. Commun.* **2008**, 4875−4884.
(13) Brookhart, M.; Green, M. L. H.; Parkin, G. *Proc. Natl. Acad. Sci. U.S.A.* **2007**, *104*, 6908−6914.
(14) (a) Becke, A. D.; Edgecombe, K. E. *J. Chem. Phys.* **1990**, *92*, 5397−5403. (b) Silvi, B.; Savin, A. *Nature* **1994**, *371*, 683−686.
(15) (a) Silvi, B.; Fourre, I.; Alikhani, M. E. *Monatsh. Chem.* **2005**, *136*, 855−879. (b) Poater, J.; Duran, M.; Solà, M.; Silvi, B. *Chem. Rev.* **2005**, *105*, 3911−3947. (c) Silvi, B.; Gillespie, R. J.; Gatti, C. *Compr. Inorg. Chem. II* **2013**, *9*, 187−226.
(16) (a) Lepetit, C.; Silvi, B.; Chauvin, R. *J. Phys. Chem. A* **2003**, *107*, 464−473. (b) Silvi, B. *Phys. Chem. Chem. Phys.* **2004**, *6*, 256−260.
(17) Silvi, B. *J. Mol. Struct.* **2002**, *614*, 3−10.
(18) (a) Contreras-Garcia, J.; Johnson, E. R.; Keinan, S.; Chaudret, R.; Piquemal, J. P.; Beratan, D. N.; Yang, W. T. *J. Chem. Theory Comput.* **2011**, *7*, 625−632. (b) Johnson, E. R.; Keinan, S.; Mori-Sanchez, P.; Contreras-Garcia, J.; Cohen, A. J.; Yang, W. T. *J. Am. Chem. Soc.* **2010**, *132*, 6498−6506.
(19) (a) Bultinck, P.; Rafat, M.; Ponec, R.; van Gheluwe, B.; Carbó-Dorca, R.; Popelier, P. *J. Phys. Chem. A* **2006**, *110*, 7642−7648. (b) Bultinck, P.; Ponec, R.; Van Damme, S. *J. Phys. Org. Chem.* **2005**, *18*, 706−718.
(20) (a) Pilme, J.; Silvi, B.; Alikhani, M. E. *J. Phys. Chem. A* **2003**, *107*, 4506−4514. (b) Pilme, J.; Silvi, B.; Alikhani, M. E. *J. Phys. Chem. A* **2005**, *109*, 10028−10037.
(21) Castro-Rodrigo, R.; Esteruelas, M. A.; Lopez, A. M.; Oñate, E. *Organometallics* **2008**, *27*, 3547−3555.
(22) Grimme, S. *WIREs Comput. Mol. Sci.* **2011**, *104*, 211−228.
(23) Swart, M. *Chem. Phys. Lett.* **2013**, *580*, 166−171.
(24) The comparison between osmium and rhodium complexes makes sense because both metals, which are in diagonal relationship in the Periodic Table, have very similar covalent and vdW radii (1.42 and 2.00 Å and 1.44 and 2.00 Å, respectively). See http://www.ccdc.cam.ac.uk/Lists/ResourceFileList/Elemental_Radii.xlsx.
(25) Fuster, F.; Sevin, A.; Silvi, B. *J. Phys. Chem. A* **2000**, *104*, 852−858.
(26) Brayshaw, S. K.; Green, J. C.; Kociok-Köhn, G.; Sceats, E. L.; Weller, A. S. *Angew. Chem., Int. Ed.* **2006**, *45*, 452−456.
(27) Saillard, J.-Y.; Hoffmann, R. *J. Am. Chem. Soc.* **1984**, *106*, 2006−2026.
(28) Rahaman, S. M. W.; Dinda, S.; Ghatak, T.; Bera, J. K. *Organometallics* **2012**, *31*, 5533−5540.
(29) Actually, the η^2-(C,H) form can itself be regarded as a balanced symmetrical hybrid of the basic H- and C-anagostic forms. Resuming the approach based on the geometrical criterion (angle between the normal to the phenylene ring plane and the mean square coordination plane of the metal center; see section 2 and Figure 3), a simplified analysis can be proposed by discarding any reference to other centers than the key plane defined by the C, H, and metal atoms. Whatever the substituting environment of the C center is (thus possibly different from a phenylene ring), the simplified geometrical analysis takes place in the C−H−metal plane, where the following geometrical parameters are defined: d = C−H bond length (ca. 1.1 Å), h = distance of M from the C−H bond axis. α = H−C−M angle. β = C−H−M angle.Whereas

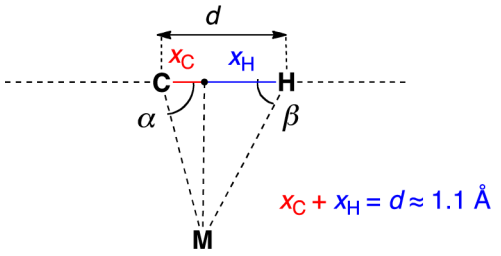

h (and less markedly d) is inversely proportional to the strength of the (CH)···M interaction, the relative H-anagostic versus C-anagostic character of the interaction can be simply appraised by $t = \cos[f_C(\alpha)]/\cos[f_H(\beta)]$, where f_C and f_H are linear functions of the angles α and β, respectively, attaining the values 90° for critical values of the angles corresponding to ideal C- and H-anagostic interactions. In any situation, the weight of the C-anagostic contribution can be thus simply estimated as

$$w_C = 1/(ct^k + 1)$$

where c is an a priori adjustable parameter (close to 1). Within this restricted model, the weight of the H-anagostic contribution is just $w_H = 1 - w_C$. In the simplest version of the model, it can just be assumed that $f_C(\alpha) = \alpha$ and $f_C(\beta) = \beta$, with the corresponding assumption being that pure C-anagostic and H-anagostic complexes correspond to $\alpha = 90°$ and $\beta = 90°$, respectively. For the sake of simplicity, it can also be assumed that $c = 1$, namely, that ideal η^2-(C,H) agostic interactions

DOI: 10.1021/acs.inorgchem.5b00069
Inorg. Chem. 2015, 54, 2960−2969

correspond to $w_C = w_H = {}^1/_2$. The resulting model is symmetrical in the α and β angles:

$$\alpha = 90° \rightarrow w_C = 1,\ w_H = 0$$

$$\beta = 90° \rightarrow w_C = 0,\ w_H = 1$$

$$\alpha = \beta \rightarrow w_C = w_H = \frac{1}{2}$$

For any metal−(CH) complex, where $0 < \alpha \leq 90°$ and $0 < \beta \leq 90°$ in the optimized geometry, the calculated values of w_C and w_H can be considered as the weights the C- and H-anagostic limiting forms. The relevance of the proposition will be inspected shortly. It is worth noting that the model can be refined in a more realistic manner. In particular, it can be more reasonably assumed that a pure C-anagostic situation corresponds to an sp^3-hybridized C atom where the critical value α_c of the α angle is no longer 90° but $\arccos[1/3] = 109.5°$. Likewise, for the H-anagostic situation corresponding to hydrogen bonding, the critical value β_c of the β angle is no longer 90° but 180°. A more complex formula is then derived, but its relevance will also be investigated for the above-described complexes (Table S5 in the SI):

$$f_C(\alpha) = \alpha - \alpha_c + 90$$

$$f_C(\beta) = \beta - \beta_c + 90$$

The distance criterion might also participate in the determination of w_C and w_H. The influence of the M···C and M···H distances can be introduced at the level of the c parameter, which thus becomes a variable, in the following way:

$$c = (MC/MH)^{k'}$$

The $k - k'$ difference of the exponents evaluates the relative importance of the angular and distance effects, and the general formula reads

$$w_C = MH^{k'} \sin^k(\beta - \beta_c)/[MC^{k'} \sin^k(\alpha - \alpha_c) + MH^{k'} \sin^k(\beta - \beta_c)]$$

For $\alpha_c = \beta_c = 90°$ and $k = k' = 1$, the denominator is equal to $MC \cos(\alpha) + MH \cos(\beta) = x_C + x_H = CH = d$, and the numerator of w_C (and w_H) is the projection of the C → M vector (and the H → M vector) on the C−H axis (with $w_C + w_H = 1$, but it is worth noting that w_C or w_H can be negative for values of the α and β angles greater that 90°).

(30) (a) Stepien, M.; Latos-Grazynski, L.; Szterenberg, L.; Panek, J.; Latajka, Z. *J. Am. Chem. Soc.* **2004**, *126*, 4566−4580. (b) Cetin, A.; Durfee, W. S.; Ziegler, C. J. *Inorg. Chem.* **2007**, *46*, 6239−6241. (c) Chang, G.-F.; Wang, C.-H.; Lu, H.-C.; Kan, L.-S.; Chao, I.; Chen, W. H.; Kumar, A.; Lo, L.; de la Rosa, M. A. C.; Hung, C.-H. *Chem.—Eur. J.* **2011**, *17*, 11332−11343.

(31) Frisch, M. J.; Trucks, G. W.; Schlegel, H. B.; Scuseria, G. E.; Robb, M. A.; Cheeseman, J. R.; Scalmani, G.; Barone, V.; Mennucci, B.; Petersson, G. A.; Nakatsuji, H.; Caricato, M.; Li, X.; Hratchian, H. P.; Izmaylov, A. F.; Bloino, J.; Zheng, G.; Sonnenberg, J. L.; Hada, M.; Ehara, M.; Toyota, K.; Fukuda, R.; Hasegawa, J.; Ishida, M.; Nakajima, T.; Honda, Y.; Kitao, O.; Nakai, H.; Vreven, T.; Montgomery, J. A., Jr.; Peralta, J. E.; Ogliaro, F.; Bearpark, M.; Heyd, J. J.; Brothers, E.; Kudin, K. N.; Staroverov, V. N.; Kobayashi, R.; Normand, J.; Raghavachari, K.; Rendell, A.; Burant, J. C.; Iyengar, S. S.; Tomasi, J.; Cossi, M.; Rega, N.; Millam, M. J.; Klene, M.; Knox, J. E.; Cross, J. B.; Bakken, V.; Adamo, C.; Jaramillo, J.; Gomperts, R.; Stratmann, R. E.; Yazyev, O.; Austin, A. J.; Cammi, R.; Pomelli, C.; Ochterski, J. W.; Martin, R. L.; Morokuma, K.; Zakrzewski, V. G.; Voth, G. A.; Salvador, P.; Dannenberg, J. J.; Dapprich, S.; Daniels, A. D.; Farkas, Ö.; Foresman, J. B.; Ortiz, J. V.; Cioslowski, J.; Fox, D. J. *Gaussian09*, revision A.1; Gaussian, Inc.: Wallingford, CT, 2009.

(32) Ehlers, A. W.; Böhme, M.; Dapprich, S.; Gobbi, A.; Höllwarth, A.; Jonas, V.; Köhler, K. F.; Stegmann, R.; Veldkamp, A.; Frenking, G. *Chem. Phys. Lett.* **1993**, *208*, 111−114.

(33) (a) te Velde, G.; Bickelhaupt, F. M.; van Gisbergen, S. J. A.; Fonseca Guerra, C.; Baerends, E. J.; Snijders, J. G.; Ziegler, T. *J. Comput. Chem.* **2001**, *22*, 931−967. (b) Fonseca Guerra, C.; Snijders, J. G.; te Velde, G.; Baerends, E. J. *Theor. Chem. Acc.* **1998**, *99*, 391−403. (c) *ADF2013, SCM, Theoretical Chemistry*; Vrije Universiteit: Amsterdam, The Netherlands, 2013; http://www.scm.com.

(34) Van Lenthe, E.; Baerends, E. J. *J. Comput. Chem.* **2003**, *24*, 1142−1156.

(35) Pye, C. C.; Ziegler, T. *Theor. Chem. Acc.* **1999**, *101*, 396−408.

(36) Bader, R. F. W. *Atoms In Molecules: A Quantum Theory*; Clarendon Press: Oxford, U.K., 1990.

(37) (a) Noury, S.; Krokidis, X.; Fuster, F.; Silvi, B. *Comput. Chem.* **1999**, *23*, 597−604. (b) Matito, E.; Silvi, B.; Duran, M.; Solà, M. *J. Chem. Phys.* **2006**, *125*, 024301. (c) Feixas, F.; Matito, E.; Duran, M.; Solà, M.; Silvi, B. *J. Chem. Theory Comput.* **2010**, *6*, 2736−2742.

(38) *Molekel 4.3* from CSCS: http://www.cscs.ch/molkel/.

(39) (a) Bultinck, P. *Faraday Discuss.* **2007**, *135*, 347−365. (b) Bultinck, P.; Rafat, M.; Ponec, R.; van Gheluwe, B.; Carbó-Dorca, R.; Popelier, P. *J. Phys. Chem. A* **2006**, *110*, 7642−7648. (c) Bultinck, P.; Fias, S.; Ponec, R. *Chem.—Eur. J.* **2006**, *12*, 8813−8818. (d) Mandado, M.; Bultinck, P.; González-Moa, M. J.; Mosquera, R. A. *Chem. Phys. Lett.* **2006**, *433*, 5−9. (e) Bultinck, P.; Ponec, R.; Carbó-Dorca, R. *J. Comput. Chem.* **2007**, *28*, 152−160. (f) Fias, S.; Damme, S. V.; Bultinck, P. *J. Comput. Chem.* **2010**, *31*, 2286−2293. (g) Fias, S.; Fowler, P. W.; Delgado, J. L.; Hahn, U.; Bultinck, P. *Chem.—Eur. J.* **2008**, *14*, 3093−3099. (h) Feixas, F.; Matito, E.; Poater, J.; Solà, M. *J. Comput. Chem.* **2008**, *29*, 1543−1554. (i) Feixas, F.; Jiménez-Halla, J. O. C.; Matito, E.; Poater, J.; Solà, M. *J. Chem. Theory Comput.* **2010**, *6*, 1118−1130. (j) Feixas, F.; Matito, E.; Duran, M.; Poater, J.; Solà, M. *Theor. Chem. Acc.* **2011**, *128*, 419−431. (k) Matito, E.; Solà, M. *Coord. Chem. Rev.* **2009**, *253*, 647−665.

(40) Matito, E.; Solà, M.; Salvador, P.; Duran, M. *Faraday Discuss.* **2007**, *135*, 325−345.

(41) Salvador, P.; Ramos-Cordoba, E. *APOST-3D*; Institute of Computational Chemistry and Catalysis, University of Girona: Catalonia, Spain, 2011.

(42) (a) Matito, E. *ESI-3D: Electron Sharing Indexes Program for 3D Molecular Space Partitioning*; Institute of Computational Chemistry and Catalysis, University of Girona: Catalonia, Spain, 2006; available from http://iqc.udg.es/~eduard/ESI. (b) Matito, E.; Duran, M.; Solà, M. *J. Chem. Phys.* **2005**, *122*, 014109. Erratum, *Ibid* **2006**, *125*, 059901.

(43) Lane, J. R.; Contreras-García, J.; Piquemal, J.-P.; Miller, B. J.; Kjaergaard, H. G. *J. Chem. Theory Comput.* **2013**, *9*, 3263−3266.

DOI: 10.1021/acs.inorgchem.5b00069
Inorg. Chem. 2015, 54, 2960−2969